Supporting information

Fine-tuning energy levels and morphology via fluorination and thermal annealing enable high efficiency non-fullerene organic solar cells

Yingying Zhao[a], Honggang Chen[a], Can Zhu[a], Jun Yuan[a], Yungui Li[b], Jiefeng Hai[c], Yunbin Hu[a], Lihui Jiang[a]*, Guohui Chen[a]*, Yingping Zou[a]

[a]College of Chemistry and Chemical Engineering, Central South University, Changsha 410083, China. *E-mail: jianglh@csu.edu.cn(L.Jiang); gh-ch@163.com(G.Chen)

[b]Max-Planck Institute for Polymer Research, Ackermannweg 10, 55128 Mainz, Germany

[c]Guangxi Key Laboratory of Electrochemical and Magneto-Chemical Functional Materials, College of Chemistry and Bioengineering, Guilin University of Technology, Guilin 541004, China

1. General measurement

^{1}H NMR and ^{13}C NMR spectra were measured with Bruker AM 400 and AM 500 spectrometers. UV-Vis absorption spectra were recorded on a SHIMADZU UV-2600 spectrophotometer. Cyclic voltammetry curves were measured by CHI660E electrochemical workstation. Its external system consists of three electrodes, of which Ag/AgCl as the reference electrode, platinum wire as the counter electrode, and platinum plate as the working electrode. The measurements were performed in an anhydrous argon-saturated solution of 0.1 M tetrabutylammonium hexafluorophosphate (Bu_4NPF_6) in in acetonitrile. The *EQE* spectra were measured by Solar Cell Spectral Response Measurement System QE-R301. The *J-V* curves were measured through the Keithley 2400 Source-Measure Unit in high purity nitrogen-filled glove box. The AFM images were explored through SPI 3800N atomic force microscopy. The TEM images were obtained by the JEM-1011 transmission electron microscope. The hole and electron mobilities of OSCs were obtained through the space charge limited current (SCLC) method. The charge carrier mobilities were calculated through the MOTT-Gurney formula:

$$J = \frac{9\varepsilon_r\varepsilon_0\mu V_{eff}^2}{8L^3}$$

In which J is the current density, ε_r is the relative dielectric constant, ε_0 is the vacuum dielectric constant, μ is the charge carrier mobility, V_{eff} is the applied voltage, L is the thickness of active layer.

2. Fabrication of OSCs

Inverted OSCs were fabricated with the structure of ITO/ZnO/active layers/MoO_3/Ag. The ITO-coated glass substrate was cleaned with deionized water, acetone, and isopropanol in order, and then processed in an ultraviolet-ozone chamber in for 20 min. The ZnO precursor solution was spin coated on the ITO substrate at 4000 rpm for 40 s, then treated in the air at 150 °C for 15 min. The PM6 and TPQx-4F (or TPQx-6F) (16 mg mL^{-1}) was dissolved in CF, and which was spin coated onto the ZnO layer at 3000 rpm for 30 s. After spin-coating, the layer active was annealed at different temperatures for 5 min. Finally, the device was obtained through thermal deposition of 10 nm MoO_3 layer and 100 nm Ag electrode.

3. Materials and Synthesis

Unless otherwise specified, all medicines are purchased from Sigma-Aldrich or Acros Inc. and used directly without purification. All the reagents and solvents used in the experiment are analytical purity and are used directly without purification. PM6 (Mn =49 kDa) was purchased from Solarmer Energy Inc. 2-(5,6-difluoro-3-oxo-2,3-dihydro-1H-inden-1-ylidene)malononitrile was purchased from Derthon OPV Co Ltd; 12, 13-bis(2-ethylhexyl)-3, 9-diundecyl-12, 13-dihydro[1]thiadiazole[2]thieno[2”, 3”:4, 5]thieno[2’3’:4, 5]pyrrolo[3, 2-g]thieno[2’,3’:4, 5]thieno[3, 2-b]indole and 1,2-Bis(5-(2-ethylhexyl)-4-fluorothiophen-2-yl)ethane-1,2-dione were synthesized according to the literature report.

13-(2-ethylhexyl)-6,7-bis[5-(2-ethylhexyl)-4-fluorothiophen-2-yl]-14-(2-propylhexyl)-3,10-diundecyl13,14Dihydrobisthieno[2'',3'':4',5']thieno[2',3':4,5] pyrrolo[3,2-f:2',3'-h]quinoxaline(2)

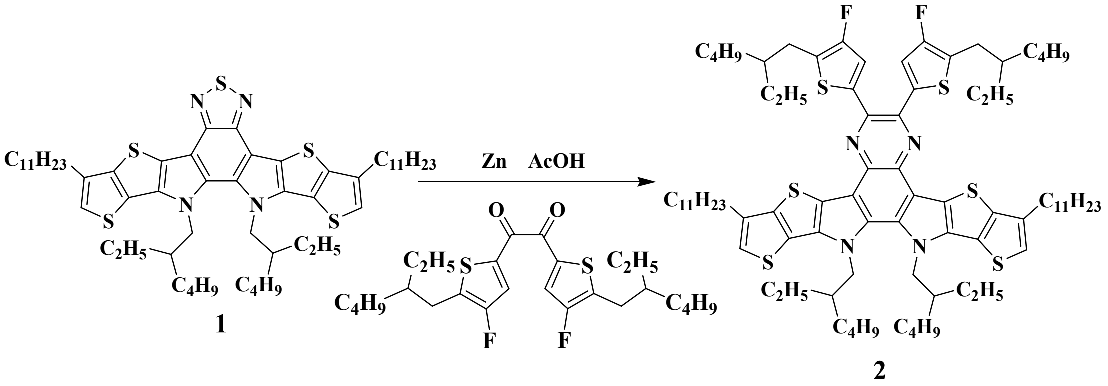

To a solution of compound **1** (1.457 g, 1.5 mmol) in acetic acid (70 mL) was added zinc powder (1.962 g, 30 mmol) in one portion. Then the mixture solution was heated to 140 °C for 15 min. After the solution was cooled at room temperature, the solid was removed by filtration. The mixture solution was extracted with ethyl acetate (500 mL ×3) and sodium hydroxide solution until the organic layer was basic. The combined organic layer was dried over $MgSO_4$. After removal of the solvent under reduced pressure, a yellow liquid was obtained without further purification. To a solution of yellow liquid in acetic acid (80 mL) in three flasks at room temperature. Then 1,2-Bis(5-(2-ethylhexyl)-4-fluorothiophen-2-yl)ethane-1,2-dione and acetic acid (50 ml) are put into the constant pressure dropping funnel. The resulting mixture was heated to 90 °C, drop the mixture in the constant pressure dropping funnel into three bottles and stir it overnight at 125 °C. After cooling to room temperature, the reaction mixture was quenched by sodium bicarbonate solution, then extracted with dichloromethane (100 mL×3) and water (150 mL). The combined organic layer was dried over $MgSO_4$. After removal of the solvent under reduced pressure, the residue was purified by column chromatography on silica gel (petroleum ether/dichloromethane, v/v, 10/1) to give the yellow solid **2**. (0.50 g, 36 %).

^{1}H NMR (400 MHz, $CDCl_3$) δ 7.24 (s, 2H), 7.02 (s, 2H), 4.64 (s, 4H), 2.85 (dd, *J* = 16.2, 7.3 Hz, 8H), 2.05-1.85 (m, 8H), 1.74 (s, 2H), 1.52-1.33 (m, 36H), 1.03-0.84 (m, 44H), 0.63 (dd, *J* = 15.4, 5.7 Hz, 12H).

14-(2-ethylhexyl)-6,7-bis[5-(2-ethylhexyl)-4-fluorothiophen-2-yl]-11-methyl-13-[2-(2-oxoethyl)hexyl]-3,10-diundecyl-13,14Dihydrobisthieno[2'',3'':4',5']thieno[2',3':4,5]pyrrolo[3,2-f:2',3'-h]quinoxaline-2-carbaldehyde(3)

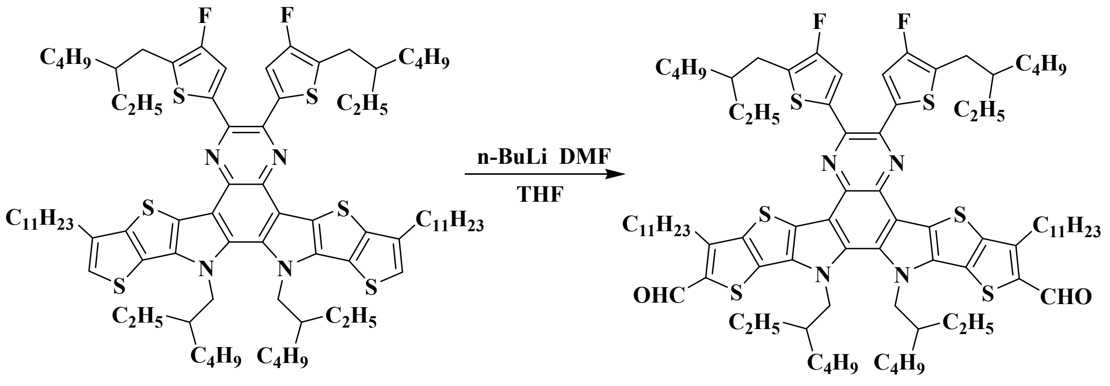

2 **3**

To a solution of compound **2** (0.694 g, 0.50 mmol) in THF (20 mL) at -78 °C, n-BuLi (0.2 mL, 2.5 M in hexane) was added dropwise slowly under nitrogen. After stirring at−78 °C for 1.5 h. Then dry DMF (0.12 mL, 3.66 mmol) was added at the mixture at −78 °C, and then the mixing continued for another 30 min at −78 °C. Next, the reaction mixture was warmed to room temperature and stirred overnight. After 12 h, the mixture was poured into water and extracted with dichloromethane to afford the crude product. The crude product was purified by column chromatography on a silica gel using hexane as eluent. The reaction mixture was poured into water, and then extracted with dichloromethane twice. The combined organic layer was washed with water and brine, dried over $MgSO_4$, and evaporated under reduced pressure. The crude product was purified with column chromatography on silica gel using dichloromethane/petroleum ether (1/1, v/v) as the eluent to give a yellow solid **3** (0.867 g, 60% yield).

^{1}H NMR (400 MHz, $CDCl_3$) δ 10.15 (s, 2H), 7.27 (s, 2H), 4.67 (t, *J* = 7.8 Hz, 4H), 3.24 (t, *J* = 7.5 Hz, 4H), 2.84 (d, *J* = 6.6 Hz, 4H), 2.12-1.85 (m, 8H), 1.77-1.72 (m, 2H), 1.54-1.31 (m, 36H), 1.11-0.84 (m, 44H), 0.65 (dd, *J* = 11.8, 6.7 Hz, 12H).

TPQx-6F

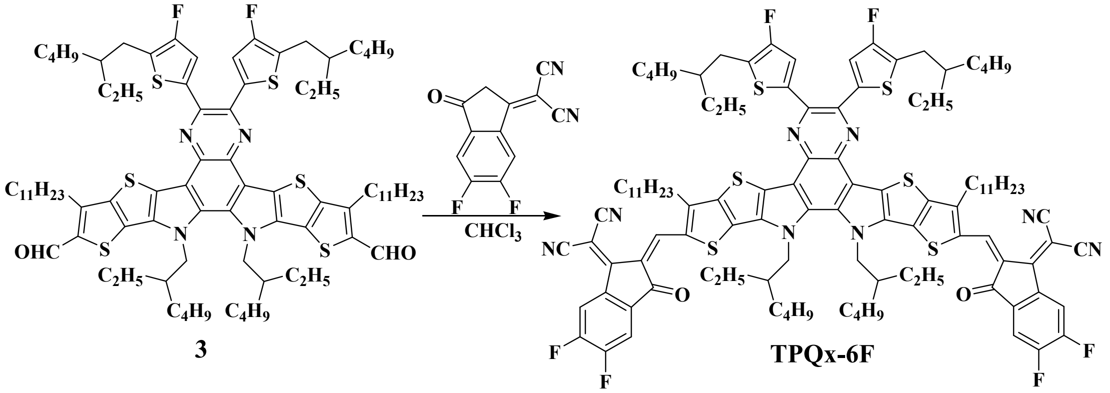

Compound **3** (0.217 g, 0.15 mmol), 2-(5, 6-difluoro-3-oxo-2,3-dihydro-1H-inden-1-ylidene) malononitrile (0.21 g, 0.90 mmol), pyridine (1 mL) and chloroform (50 mL) were dissolved in a round bottom flask under nitrogen. The mixture was stirred at 65 °C overnight. After cooling to room temperature, the mixture was poured into methanol and filtered. The residue was purified with column chromatography on silica gel using dichloromethane/petroleum ether (1/1, v/v) as the eluent to receive a dark blue solid **TPQx-6F** (0.157 g, 56% yield).

^{1}H NMR (400 MHz, $CDCl_3$) δ 9.17 (s, 2H), 8.60-8.52 (m, 2H), 7.72 (t, *J* = 7.2 Hz, 2H), 7.33 (s, 2H), 4.82 (s, 4H), 3.30 (s, 4H), 2.88 (d, *J* = 6.2 Hz, 4H), 2.18 (s, 2H), 1.99-1.73 (m, 8H), 1.64-1.34 (m, 36H), 1.26 (s, 44H), 0.76 (d, *J* = 24.7 Hz, 12H).

The synthetic method for **TPQx-4F** is similar to the above.

4. Spectral Charts of NMR

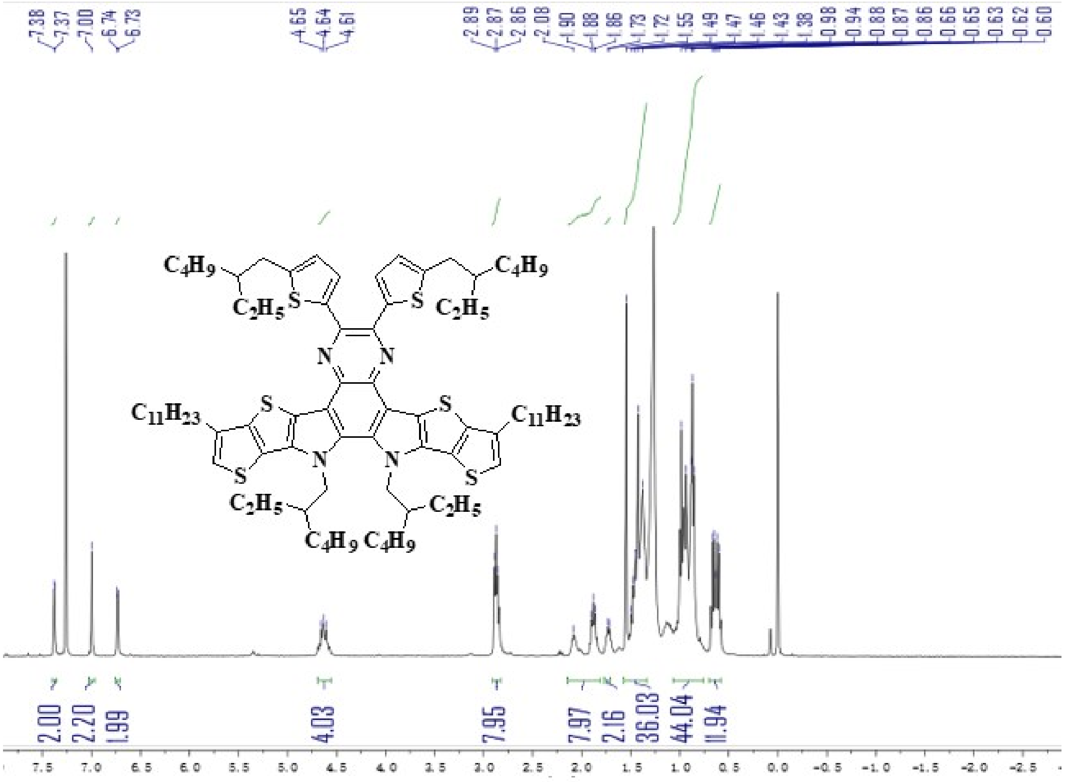

Figure S1. ^{1}H NMR spectrum of 13,14-bis(2-ethylhexyl)-6,7-bis(5-(2-ethylhexyl)-4-fluorothiophen-2-yl)-3,10-diundecyl-13,14-dihydrothieno[2",3":4',5']thieno[2',3':4,5] pyrrolo[3,2-f]thieno[2",3":4',5']thieno[2',3':4,5]pyrrolo[2,3-h]quinoxaline

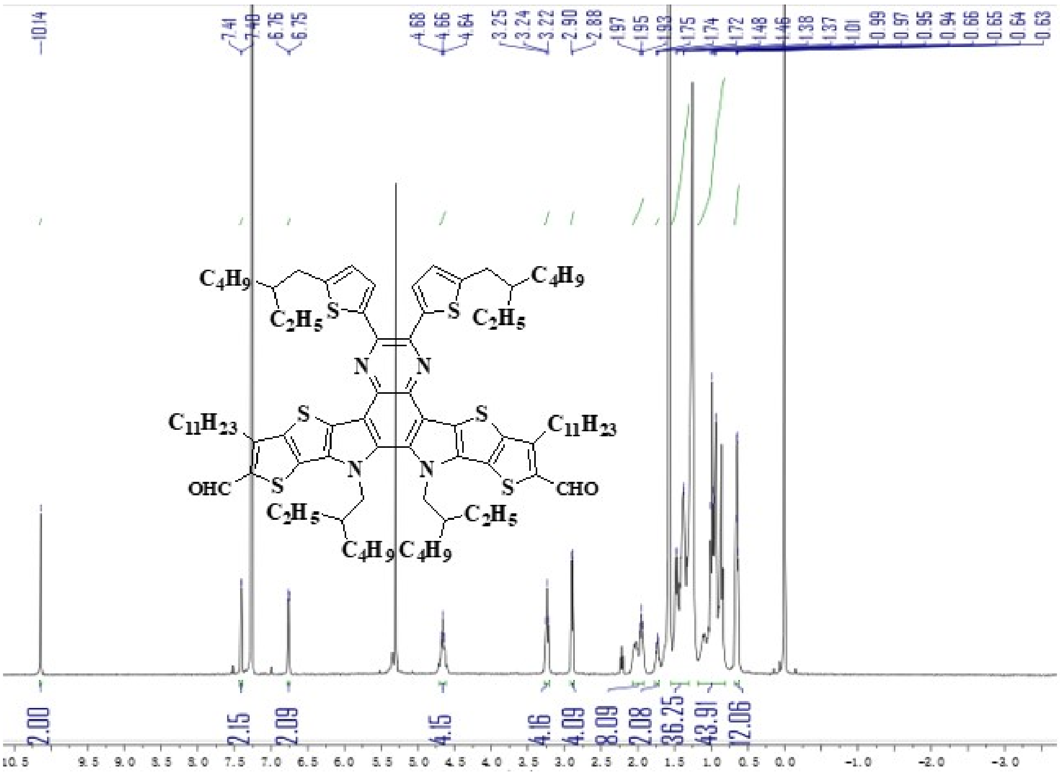

Figure S2. ^{1}H NMR spectrum of 13,14-bis(2-ethylhexyl)-6,7-bis(5-(2-ethylhexyl)thiophen-2-yl)-3,10-diundecyl-13,14-dihydrothieno[2'',3'':4',5']thieno[2',3':4,5]pyrrolo[3,2-f]thieno[2'',3'':4',5']thieno[2',3':4,5]pyrrolo[2,3-h]quinoxaline-2,11-dicarbaldehyde

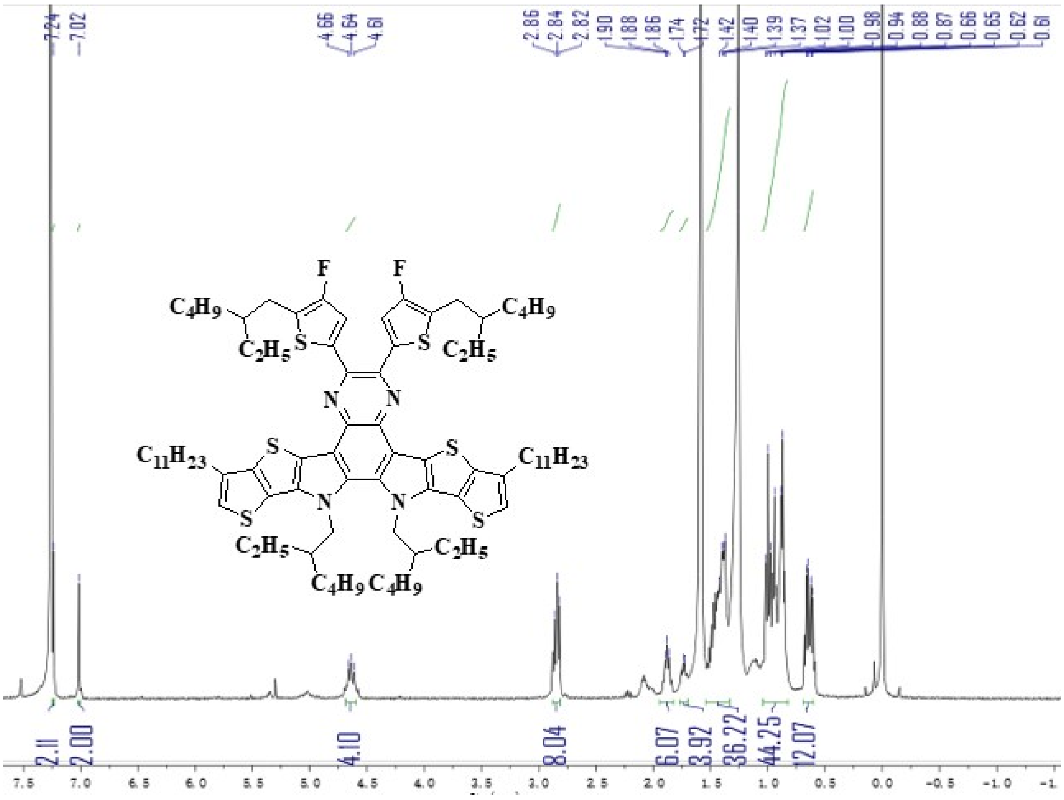

Figure S3. ^{1}H NMR spectrum of 13-(2-ethylhexyl)-6,7-bis[5-(2-ethylhexyl)-4-fluorothiophen-2-yl]-14-(2-propylhexyl)-3,10-diundecyl13,14dihydrobisthieno [2'',3'':4',5']Thieno[2',3':4,5]pyrrolo[3,2-f:2',3'-h]quinoxaline

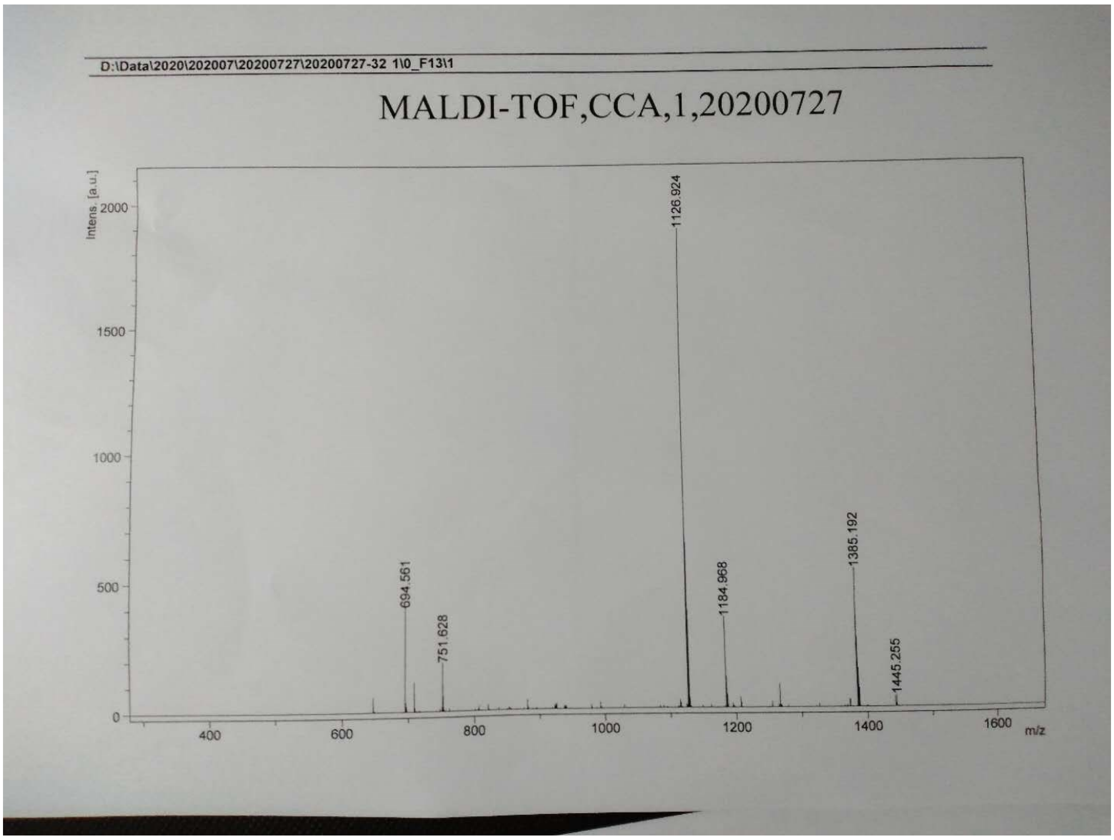

Figure S4. Mass spectrometer of 13-(2-ethylhexyl)-6,7-bis[5-(2-ethylhexyl)-4-fluorothiophen-2-yl]-14-(2-propylhexyl)-3,10-diundecyl-13,14-dihydrobisthieno [2'',3'':4',5']thieno[2',3':4,5]pyrrolo[3,2-f:2',3'-h]quinoxaline

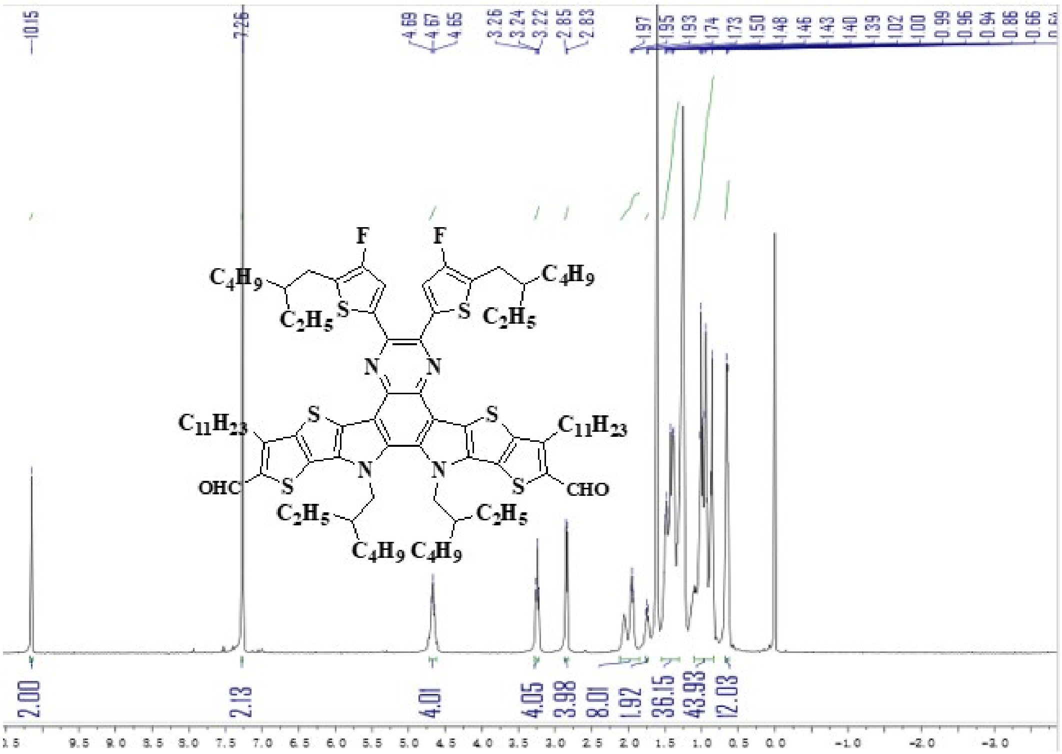

Figure S5. ^{1}H NMR spectrum of 14-(2-ethylhexyl)-6,7-bis[5-(2-ethylhexyl)-4-fluorothiophen-2yl]-11-methyl-13-[2-(2-oxoethyl)hexyl]-3,10-diundecyl-13,14-dihydrobisthieno[2",3":4',5']thieno[2',3':4,5]pyrrolo[3,2-f:2',3'-h]quinoxaline-2-carbaldehyde

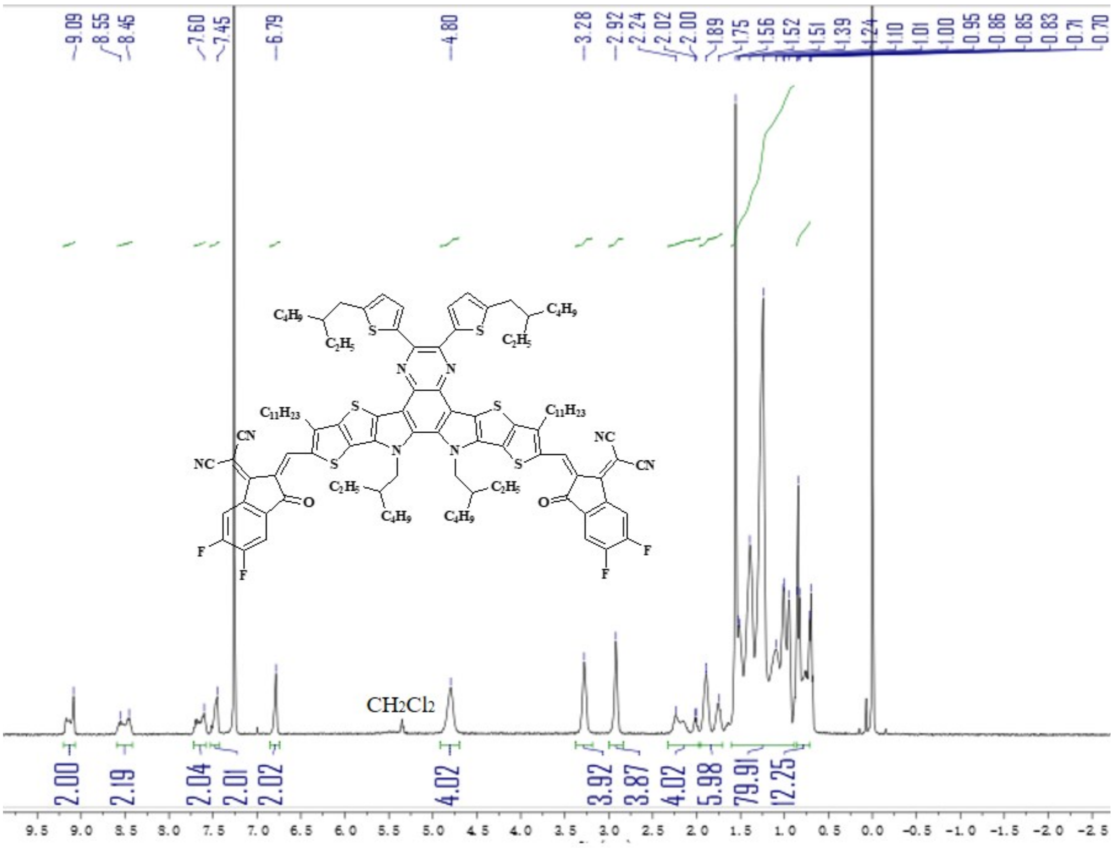

Figure S6. ^{1}H NMR spectrum of TPQx-4F.

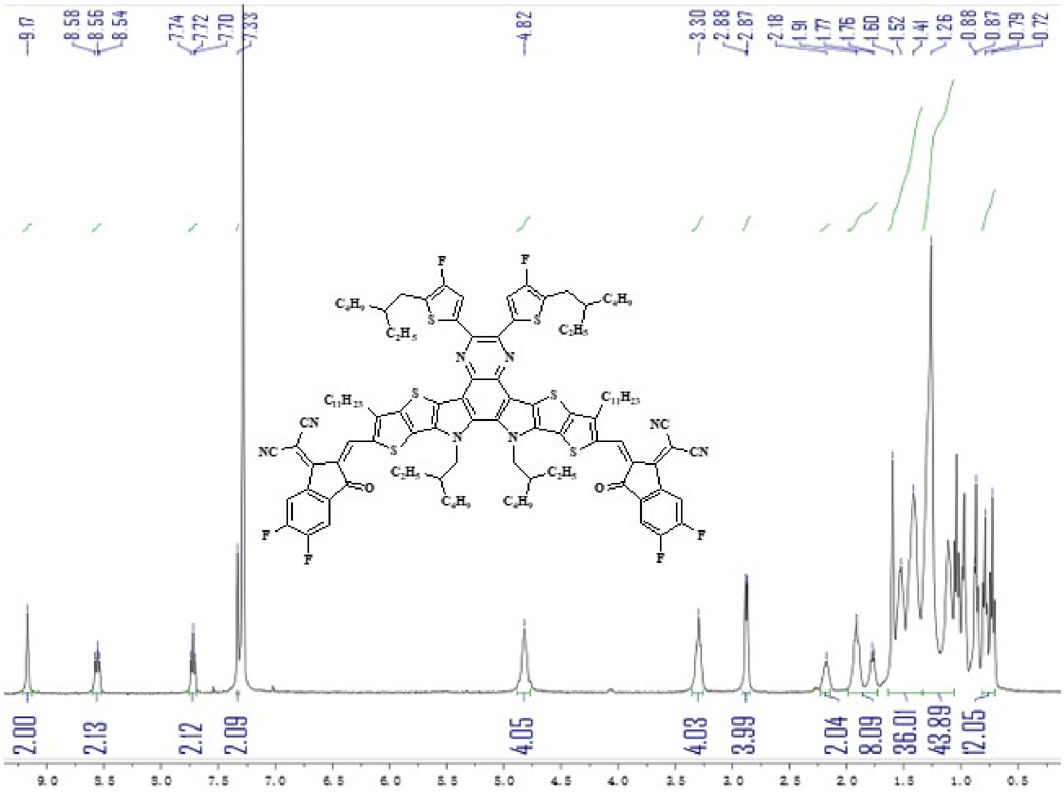

Figure S7. ^{1}H NMR spectrum of TPQx-6F.

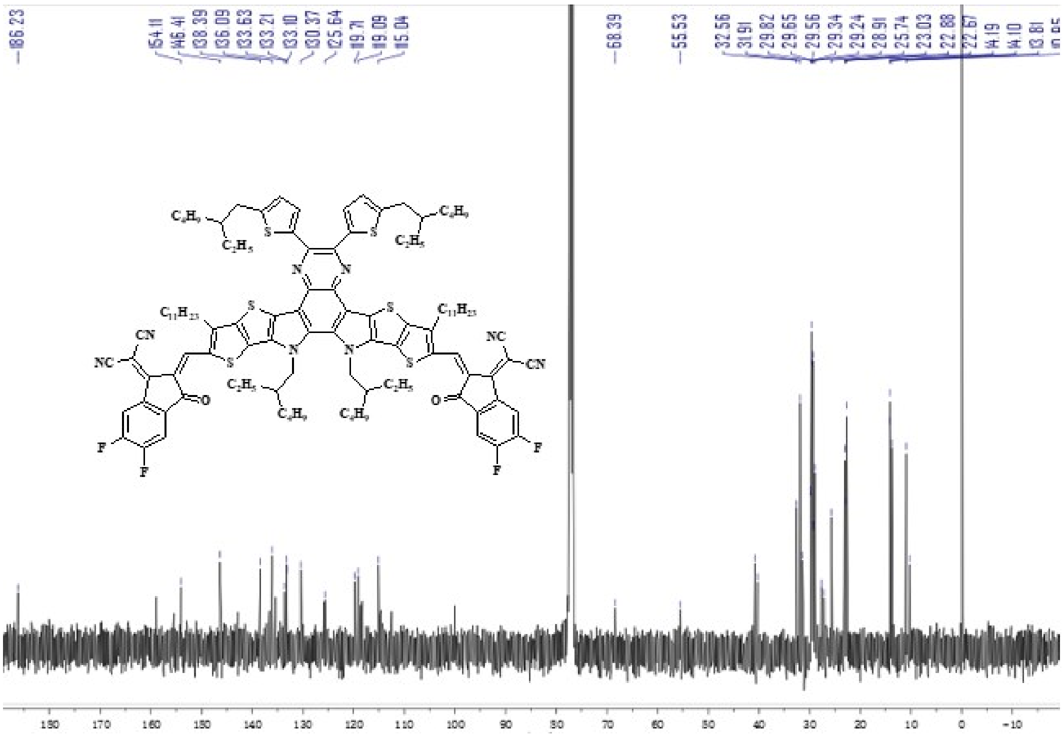

Figure S8. ^{13}C NMR spectrum of TPQx-4F.

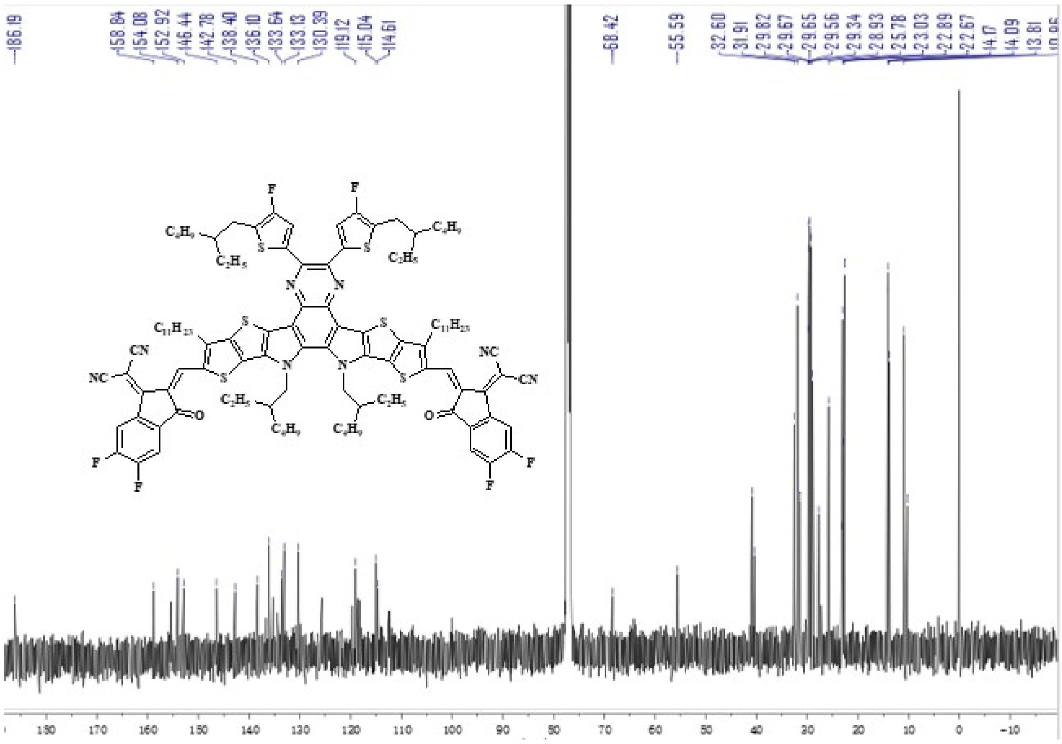

Figure S9. ^{13}C NMR spectrum of TPQx-6F.

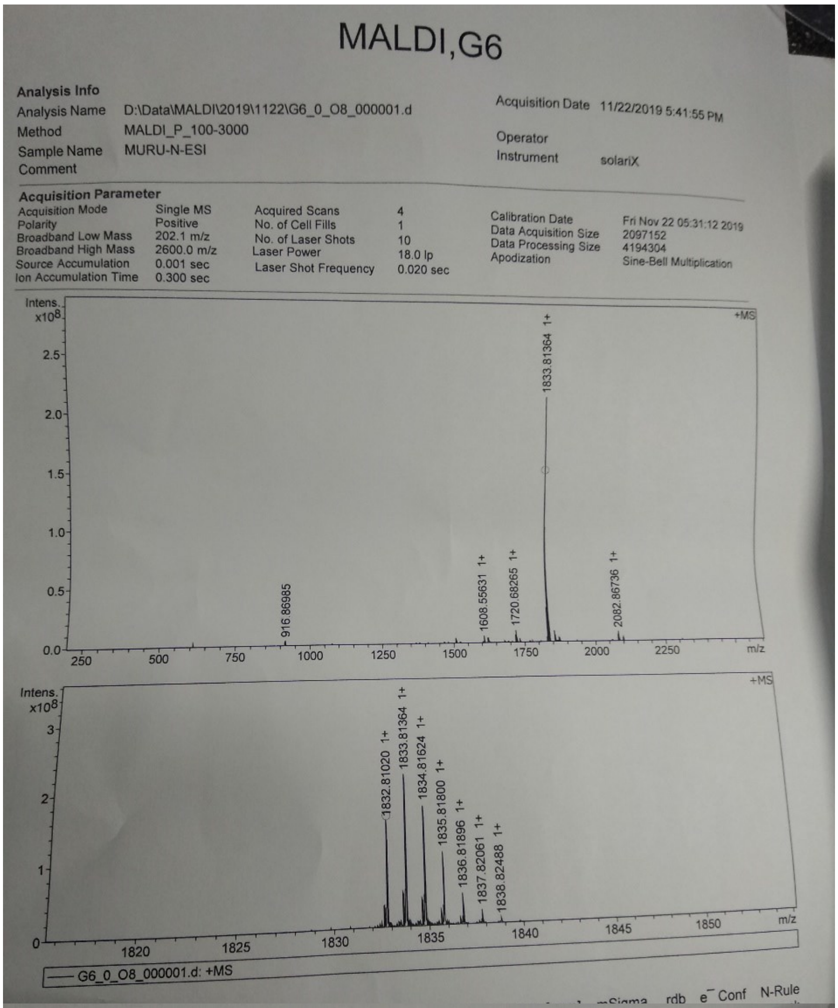

MALDI,G6

Analysis Info

Analysis Name	D:\Data\MALDI\2019\1122\G6_0_O8_000001.d
Method	MALDI_P_100-3000
Sample Name	MURU-N-ESI
Comment	
Acquisition Date	11/22/2019 5:41:55 PM
Operator	
Instrument	solariX

Acquisition Parameter

Acquisition Mode	Single MS	Acquired Scans	4	Calibration Date	Fri Nov 22 05:31:12 2019
Polarity	Positive	No. of Cell Fills	1	Data Acquisition Size	2097152
Broadband Low Mass	202.1 m/z	No. of Laser Shots	10	Data Processing Size	4194304
Broadband High Mass	2600.0 m/z	Laser Power	18.0 lp	Apodization	Sine-Bell Multiplication
Source Accumulation	0.001 sec	Laser Shot Frequency	0.020 sec		
Ion Accumulation Time	0.300 sec				

mSigma rdb e⁻ Conf N-Rule

Figure S1

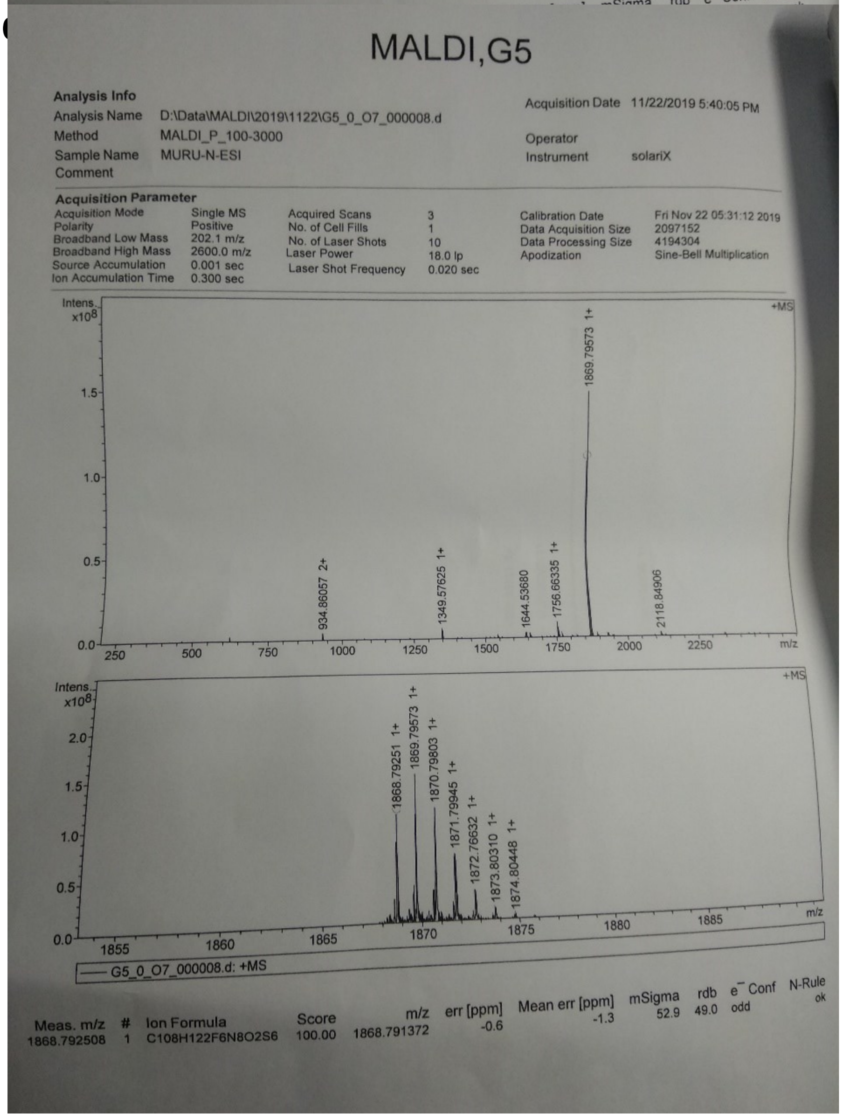

MALDI,G5

Analysis Info

Analysis Name	D:\Data\MALDI\2019\1122\G5_0_O7_000008.d
Method	MALDI_P_100-3000
Sample Name	MURU-N-ESI
Comment	
Acquisition Date	11/22/2019 5:40:05 PM
Operator	
Instrument	solariX

Acquisition Parameter

Acquisition Mode	Single MS	Acquired Scans	3	Calibration Date	Fri Nov 22 05:31:12 2019
Polarity	Positive	No. of Cell Fills	1	Data Acquisition Size	2097152
Broadband Low Mass	202.1 m/z	No. of Laser Shots	10	Data Processing Size	4194304
Broadband High Mass	2600.0 m/z	Laser Power	18.0 lp	Apodization	Sine-Bell Multiplication
Source Accumulation	0.001 sec	Laser Shot Frequency	0.020 sec		
Ion Accumulation Time	0.300 sec				

Meas. m/z	#	Ion Formula	Score	m/z	err [ppm]	Mean err [ppm]	mSigma	rdb	e⁻ Conf	N-Rule
1868.792508	1	$C_{108}H_{122}F_6N_8O_2S_6$	100.00	1868.791372	-0.6	-1.3	52.9	49.0	odd	ok

Figure S11. Mass spectrometer of TPQx-6F.

5. Thermal, optical and photovoltaic data

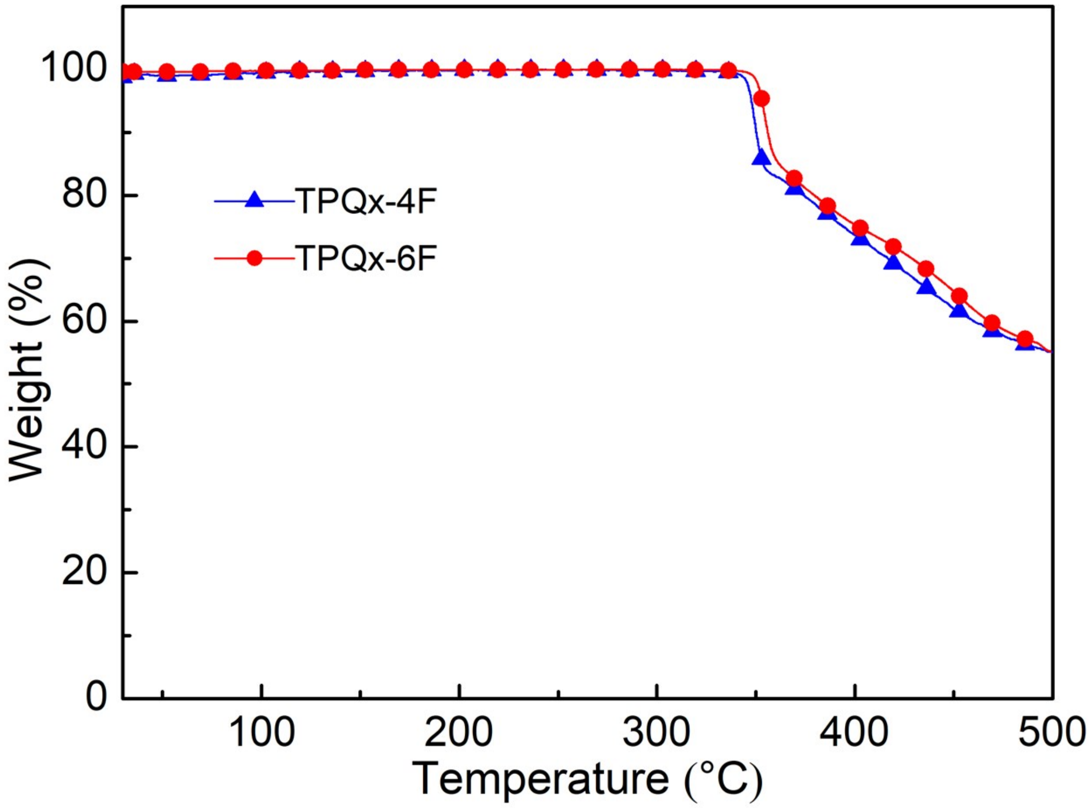

Figure S12. TGA curves of the TPQx-4F and TPQx-6F.

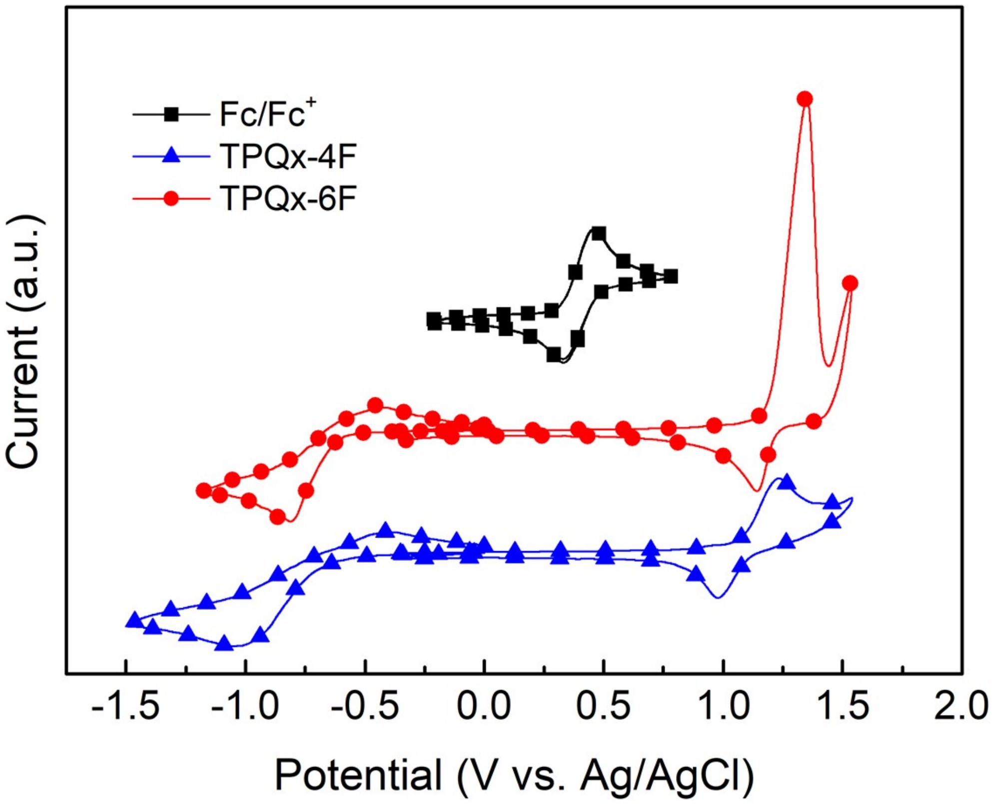

Figure S13. Cyclic voltammetry curves for neat films of TPQx-4F and TPQx-6F.

Table S1. The photovoltaic performance of the devices with different ratio of PM6:TPQx-6F.

Ratio	Annealing (°C)	V_{oc} (V)	J_{sc} (mA cm^{-2})	FF (%)	PCE (%)
1:1	100, 5min	0.92	20.93	72.02	13.86
1:1.2		0.92	21.97	72.16	14.62
1:1.4		0.91	21.54	68.66	13.41
1:1.8		0.90	20.83	71.12	13.35

Table S2. The photovoltaic performance of the PM6:TPQx-6F blends under different annealing temperature.

Ratio	Annealing (°C)	V_{oc} (V)	J_{sc} (mA/cm^2)	FF (%)	PCE (%)
1:1.2	60	0.92	20.91	72.25	13.90
	80	0.91	20.20	72.44	14.12

	100	0.92	21.54	72.16	14.62
	120	0.91	21.72	72.25	14.00

Table S3. The photovoltaic performance of PM6:TPQx-6F blends with different film thickness.

Ratio	thickness (nm)	V_{oc} (V)	J_{sc} (mA/cm^2)	FF (%)	PCE (%)
1:1.2	50	0.91	21.23	70.96	13.70
	75	0.92	22.37	72.16	14.62
	105	0.90	22.47	70.20	14.22
	150	0.90	21.77	68.69	13.49
	210	0.89	21.67	62.44	12.04

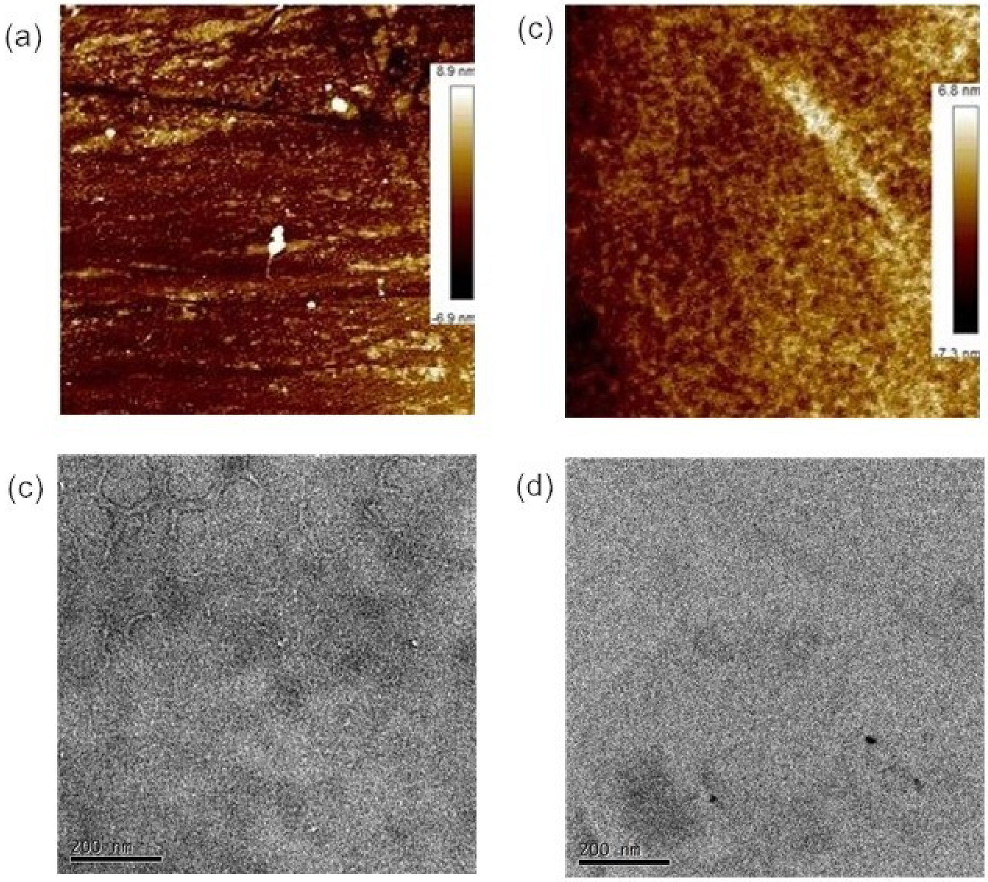

Fig. S14. The AFM (5 μm×5 μm scale) images of the as cast (a) PM6:TPQx-4F and (b) PM6:TPQx-6F blend films. The TEM images of the as cast (c) PM6:TPQx-4F and (d) PM6:TPQx-6F blend films.